
Broadband Quad-Element MIMO Antenna with Enhanced Isolation for Sub-6 GHz and Sub-7 GHz 5G Applications**Mya Sandar Aung¹, Tin Tin Hla²**myasandaraung.ec@gmail.com, tintinhla99@gmail.com^{1,2} Department of Electronic Engineering, Mandalay Technological University, Myanmar

Article Information

Submitted : 12 May 2024

Reviewed: 15 May 2024

Accepted : 15 Jun 2024

KeywordsMonopole Antenna,
MIMO, Broadband,
Enhanced Isolation, 5G

Abstract

In this manuscript, a broadband quad-element MIMO antenna with enhanced isolation for n77, n78, and n79 bands of Sub-6 GHz and the n46 and n96 bands of Sub-7 GHz under 5G applications is designed. The designed antenna element is a rectangular monopole antenna comprising a semi-circular cut and a semi-circle embedded to obtain a wide bandwidth. These four-element antennas are aligned orthogonally to achieve the compact size and high isolation features of MIMO performance. The overall area of MIMO antenna is $40 \times 40 \times 1.6 \text{ mm}^3$. MIMO antenna has a high isolation of $< -21 \text{ dB}$, an envelope correlation coefficient ($\text{ECC} < 0.0002$), a high diversity gain ($\text{DG} > 9.99$), an MEG gain of -3 dB , and a peak gain of 5.08 dBi . The results of the experiment are satisfactory with the S-parameter simulation results. According to the results, a broadband quad-element MIMO antenna is a suitable candidate for Sub-6 GHz and Sub-7 GHz 5G applications.

A. Introduction

Mobile communication technology has evolved significantly over the years. From the first generation (1G) to the current fifth-generation (5G), each new iteration has brought about substantial changes in terms of speed, capacity, and connectivity. Each generation has introduced new features and capabilities, revolutionizing the way we communicate and access information. The transition to 5G promises to deliver even faster speeds, lower latency, and higher capacity than its predecessors. With 5G technology, users will experience a more seamless and interconnected network that will enable faster download and upload speeds, support more connected devices, and unlock new opportunities for industries such as IoT, self-driving cars, and virtual reality [1]. The 3GPP Release-15 NR specifications designate the 5G NR band's middle band (C-band) as band n77 (3300-4200) MHz, n78 (3300-3800) MHz, and band n79 (4400-5000) MHz. The new 3GPP Release-16 standards have recommended the new radio access technology known as 5G NR Unlicensed (5G NR-U) band which intends to expand the 5G NR band n77/n78/n79 to the unlicensed band 5G NR-n96 (5925 -7125) MHz and 5G NR-U band n46 (5150–5925 MHz)[2]. MIMO (Multiple-Input Multiple-Output) technology provides a real breakthrough for wireless communication and is based on the use of multiple antennas for transmitting and receiving data. MIMO systems use several antennas at the two ends of the link as opposed to a single antenna and thereby achieve higher data rates and better spectral efficiency. MIMO technology improves signals by eliminating fading and interference and as a result, it more dependable wireless connections. MIMO technology used for the 5G network makes it possible to extend coverage, add capacity, and improve network performance. Generally, MIMO technology is a key enabler of wireless communication and of future high-data-rate transmissions and efficient network operation [3].

In [4], a 4-port MIMO antenna using a common radiator on a flexible substrate is discussed for Sub-1GHz, Sub-6GHz 5G NR, and Wi-Fi 6 applications. A novel microstrip patch antenna is designed using slots and parasitic strips to operate at sub-6 GHz and Sub-7 GHz under 5G. [5]. It has been reported that wideband MIMO antenna designs for smartphone applications include the 5G NR n77, n78, and n79 bands, in addition to the WLAN-5 GHz band (5150–5825 MHz). [6]. In [7], the construction of a dual-band antenna with 12 monopole elements is investigated for 5G smartphone applications. In [8], a wideband MIMO antenna with four pairs of compact microstrip-fed slot antennas provides good isolation, great efficiency, and minimum correlation among the antennas, as suggested. In [9], a compact four-port MIMO antenna design for Sub-6 GHz and IoT applications, achieving good isolation and wideband characteristics, is presented. Four monopole antennas with a circular patch and four L-shaped branch decoupling structures are designed to enhance bandwidth and high isolation for WLAN/5G/WiFi applications, as discussed in [10]. The development of a compact 4-port MIMO antenna system is designed for 5G band n77 mobile terminals [11]. The design of low-profile wideband conjoined open-slot antennas fed by grounded coplanar waveguides for 4x4 5G MIMO operation is presented. [12]. A compact four-port multiple input, multiple output antenna system for 3.5 GHz 5G technology is presented [13]. The

two-port circular MIMO antenna with round cuts integrates metamaterials to improve gain and isolation for mmwave 5G smartphone applications [14]. [15] presents a semi-circular UWB antenna with a semicircular slot on the top side, partial ground with triangular and rectangular slotted structures to improve impedance bandwidth, and incorporating a frequency-selective surface (FSS) layer to improve gain.

This paper presents a compact broadband quad-element MIMO antenna for 5G applications. To increase the impedance bandwidth, a single patch antenna is designed with a semi-circular cut, and semi-circular embedded. MIMO system is designed with four elements and is positioned orthogonally on an FR-4 substrate to achieve high isolation and compact size.

B. Design of Single Antenna

The single antenna design process to attain the final optimized single antenna is built up in three steps, as depicted in Figure 1. The S-parameter of design procedures is demonstrated in Figure 2. Firstly, the overall size of Antenna-1 ($A \times B \times h$) = $20 \times 20 \times 1.6 \text{ mm}^3$ is designed on the FR-4 substrate. The patch of the size is ($a \times b$) = $18 \times 10 \text{ mm}^3$ with microstrip feed of ($f_1 \times f_2$) = $2 \times 9 \text{ mm}^2$ and the ground of $g_1 \times g_2$ = $20 \times 8 \text{ mm}^2$ in Figure 1 (a). The reflection coefficient of S_{11} is $< -10 \text{ dB}$ from (4.18 GHz to 5.2 GHz). Secondly, the overall size of Antenna-2 ($C \times D \times h$) = $16 \times 16 \times 1.6 \text{ mm}^3$, and the antenna size of ($w \times l$) = $10 \times 7 \text{ mm}^2$ is designed with the modified ground of $G_1 \times G_2$ = $12 \times 6 \text{ mm}^2$. The semi-circular slot (radius, $a_1 = 2 \text{ mm}$) is trimmed from the upper center of the patch; therefore, the antenna size is more compact than Antenna-1, as depicted in Figure 1 (b). The S_{11} of Antenna-2 is improved. $S_{11} < -10 \text{ dB}$ results from (3.9 GHz to 8 GHz) in Figure 2. Finally, the semi-circle slot (radius, $a_2 = 2 \text{ mm}$) is etched on the left of the patch in Antenna-2, and the ground plane is moved to the right of the substrate in Figure 1 (c). The S-parameter of Antenna-3 is $S_{11} < -7 \text{ dB}$ for the desired frequency (3.3 GHz to 8 GHz) in Figure 2 (c).

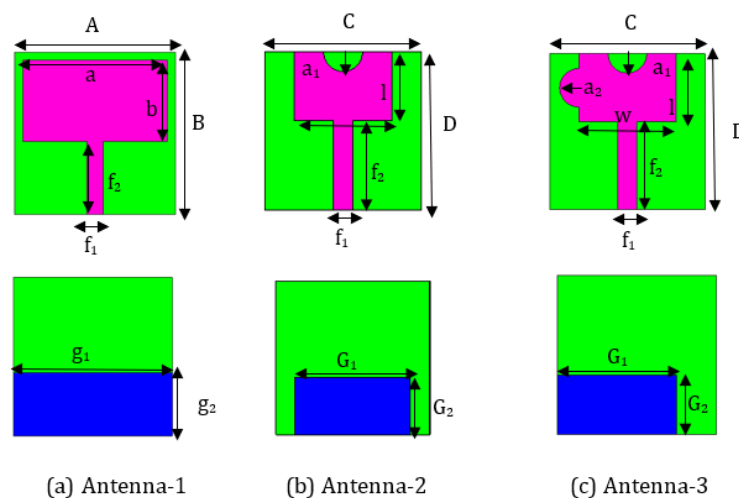


Figure 1. Design Procedure of Single Antenna

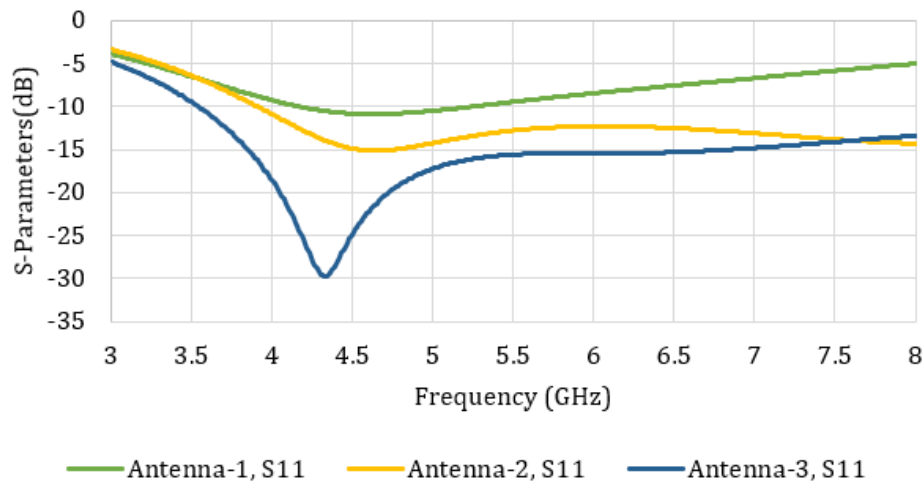


Figure 2. Compared S-parameters of Evolution of Single Antenna

The antenna parameters can be computed from the following equation [16].

$$\text{The patch width, } w = \frac{c}{2f_r \sqrt{\frac{\epsilon_r + 1}{2}}} \quad (1)$$

$$\text{The patch length, } l = L_{\text{eff}} - 2\Delta L \quad (2)$$

$$\text{The effective length, } L_{\text{eff}} = \frac{c}{2f_r \sqrt{\epsilon_{\text{reff}}}} \quad (3)$$

$$\text{The effective dielectric constant, } \epsilon_{\text{reff}} = \frac{\epsilon_r + 1}{2} + \frac{\epsilon_r - 1}{2} \left[1 + 12 \frac{h}{w} \right]^{-\frac{1}{2}} \quad (4)$$

$$\text{The extension length, } \Delta L = 0.412h \frac{(\epsilon_{\text{reff}} + 0.3) \left(\frac{w}{h} + 0.264 \right)}{(\epsilon_{\text{reff}} - 0.258) \left(\frac{w}{h} + 0.8 \right)} \quad (5)$$

$$\text{The substrate length, } L = l + 6h \quad (6)$$

$$\text{The substrate width, } W = w + 6h \quad (7)$$

$$\text{The width of feed, } f_1 = \frac{W_m}{h} \quad (8)$$

$$\text{The length of feed, } f_2 = \frac{L - l}{2} \quad (9)$$

$$\frac{W_m}{h} = \frac{8e^A}{e^{2A} - 2}; \quad \frac{W_m}{h} > 2 \text{ for } A < 1.52 \quad (10)$$

$$A = \frac{Z_0}{60} \sqrt{\frac{\epsilon_r + 1}{2} + \frac{\epsilon_r - 1}{\epsilon_r + 1} \left(0.23 + \frac{0.11}{\epsilon_r} \right)} \quad (11)$$

The radius of circular patch has been obtained in equations (12) and (13). [14]

$$a_1, a_2 = \frac{F}{\left\{ 1 + \frac{2h}{\pi \epsilon_r F} \left[\ln \left(\frac{\pi F}{2h} \right) + 1.7726 \right] \right\}^{\frac{1}{2}}} \quad (12)$$

$$F = \frac{8.791 \times 10^9}{f_r \sqrt{\epsilon_r}} \quad (13)$$

Where ;

f_r = the operating frequency

ϵ_r = dielectric constant

C. Design of Quad-Element MIMO Antenna

The reported MIMO antenna is printed on an FR-4 substrate, assumed to be 4.4, and the achieved size of MIMO antenna is $40 \times 40 \times 1.6$ mm³, as illustrated in Figure 3. The single antenna is mentioned in the previous paragraph. The prospective MIMO antenna is constructed through the orthogonal design of four monopole antennas on separate partial ground planes to obtain high isolation and compact size. The distance between the 4 elements is 11 mm in the interelement space. The prototype of MIMO antenna is depicted in Figure 5. The optimized dimensions of MIMO antenna are demonstrated in Table 1. The printed MIMO antenna is measured in S-parameters using Anritsu's Vector Network Analyzer (VNA Master MS2038C) in the Communication Laboratory Room of the Department of Electronic Engineering at Mandalay Technological University.

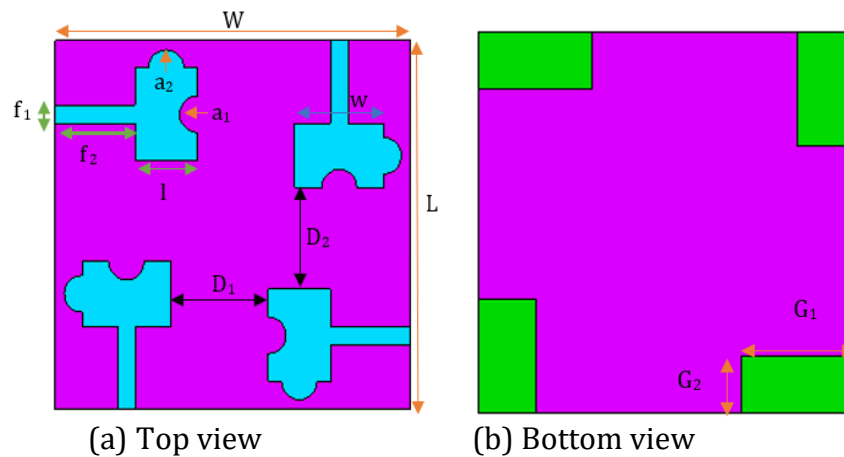


Figure 3. Geometry of Proposed quad-element MIMO Antenna

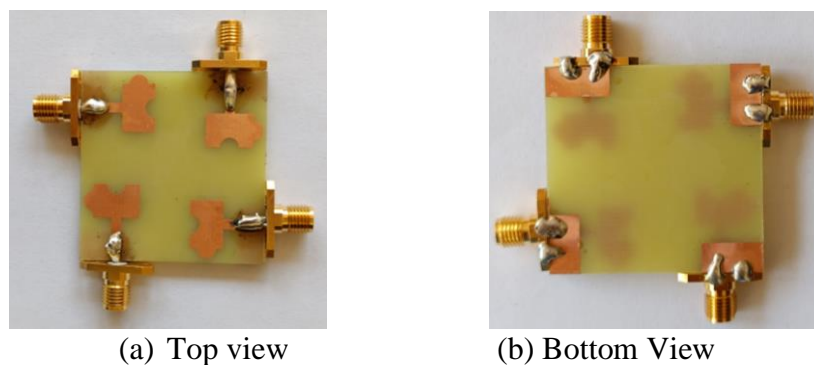


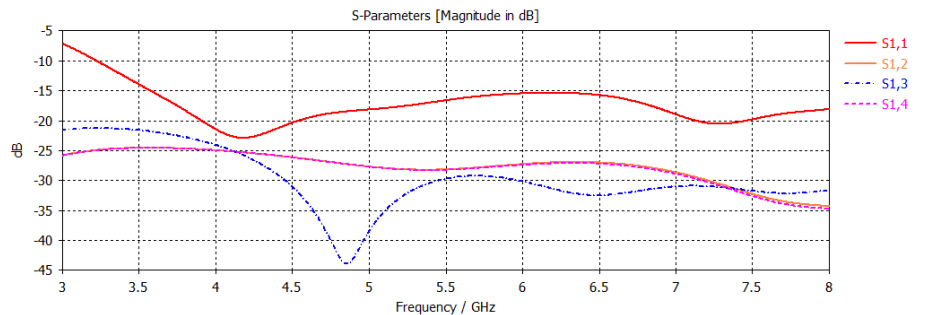
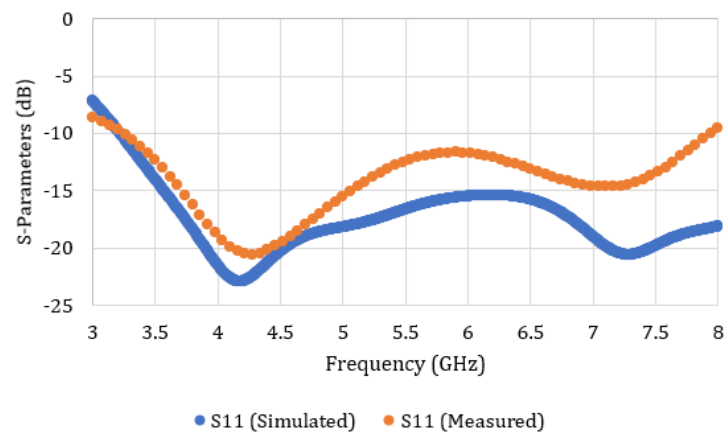
Figure 4. Prototype MIMO Antenna

Table 1. Dimensions of MIMO Antenna

Parameters	Dimensions (mm)
W	40
L	40
w	5
l	5
a ₁	2
a ₂	2
G ₁	12
G ₂	6
f ₁	2
f ₂	9
D ₁	11
D ₂	11

D. Result and Discussion

The simulated S-parameters of S_{11} , S_{12} , S_{13} , and S_{14} is demonstrated in Figure 5. The return loss $S_{11} < -11$ dB and the isolation of S_{12} , S_{13} , and S_{14} is below -21 dB. The comparison of simulated and measured results of S-parameter is depicted in Figure 6 and Figure 7. The simulation and measurement results are almost acceptable for the target frequency band (3.3-8) GHz. The isolation of measurement is better than the simulation result. Figure 8 shows the simulated gain of a MIMO antenna.

**Figure 5.** S-parameters of MIMO Antenna**Figure 6.** Comparison of S-parameter (S_{11}) Simulated and Measured of MIMO Antenna

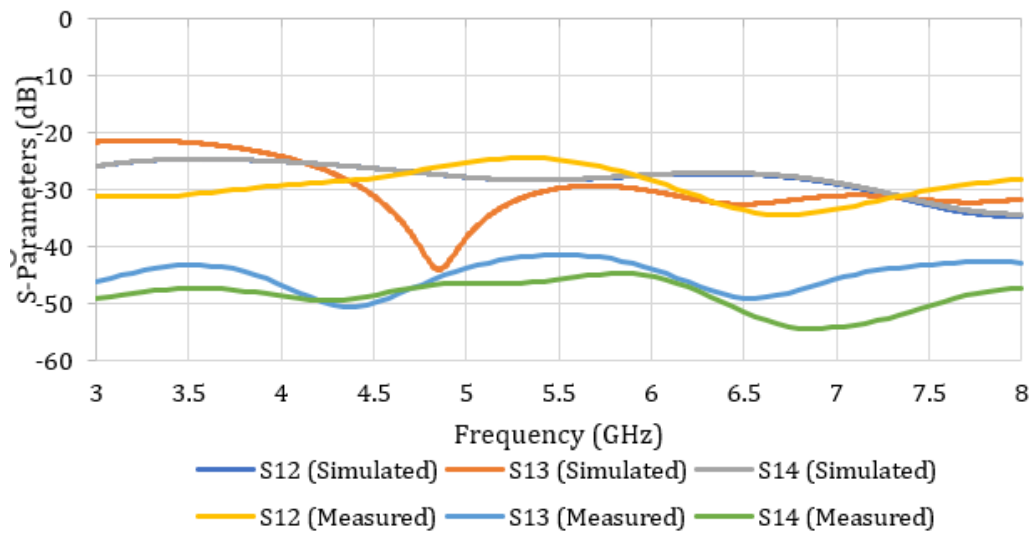


Figure 7. Comparison of S-parameter Simulated and Measured of MIMO Antenna

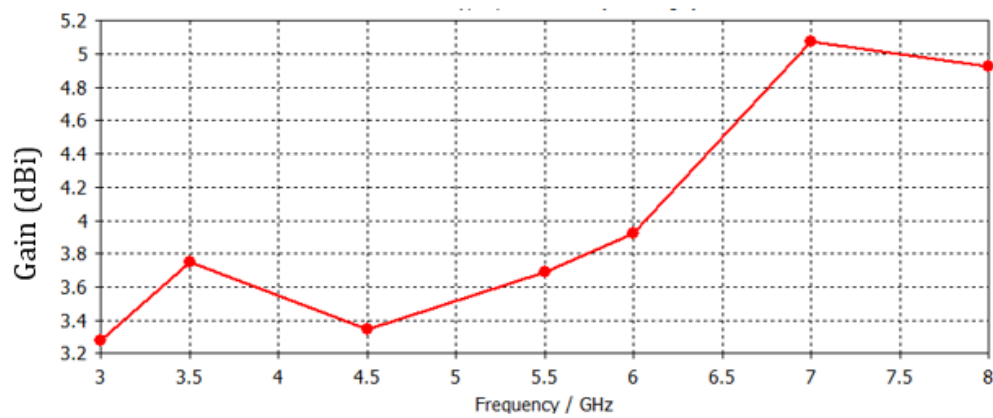


Figure 8. Simulated gain of the proposed MIMO antenna

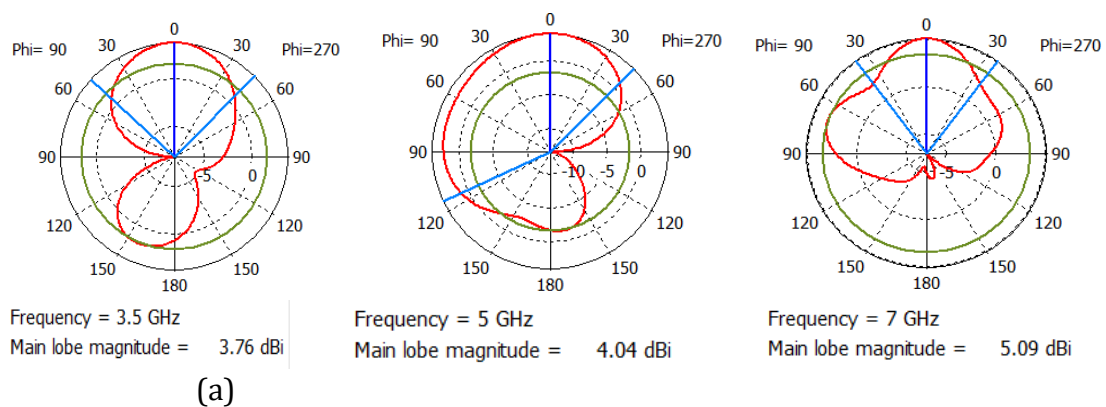


Figure 9. 2D Radiation pattern (a) 3.5GHz (b) 5 GHz (c) 7 GHz

The antenna's gain varies from 3.65 to 5.08 dBi, with a peak gain of 5.08 dBi at 7GHz. The simulation of 2D polar radiation patterns at 3.5 GHz, 5 GHz, and 7 GHz, with the gain value, is shown in Figure. 9. Fig. 10 depicts the quad-element MIMO antenna's 3D radiation pattern at 3.5 GHz, 5 GHz, and 7 GHz. The structure of the surface current on MIMO antenna is demonstrated in Figure 11. This is done by energizing Port-1 and ending the other three ports at 3.5GHz, 5GHz, and 7GHz.

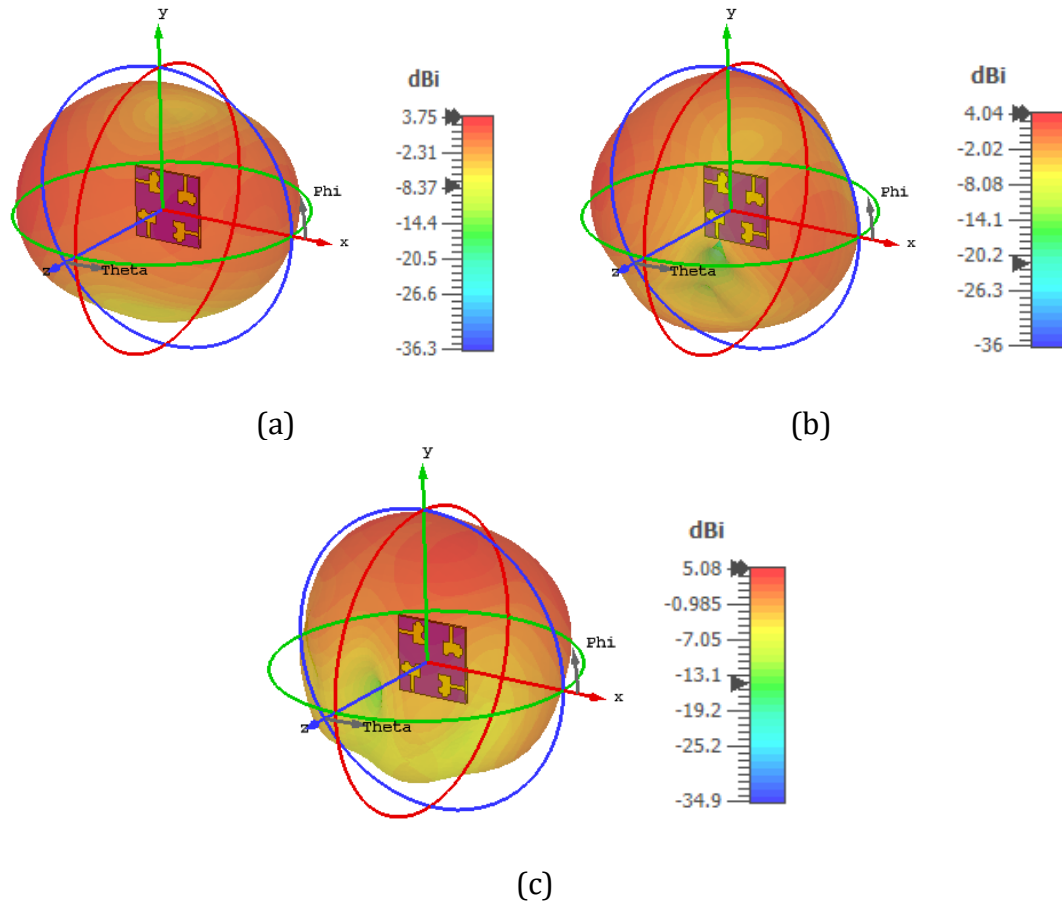
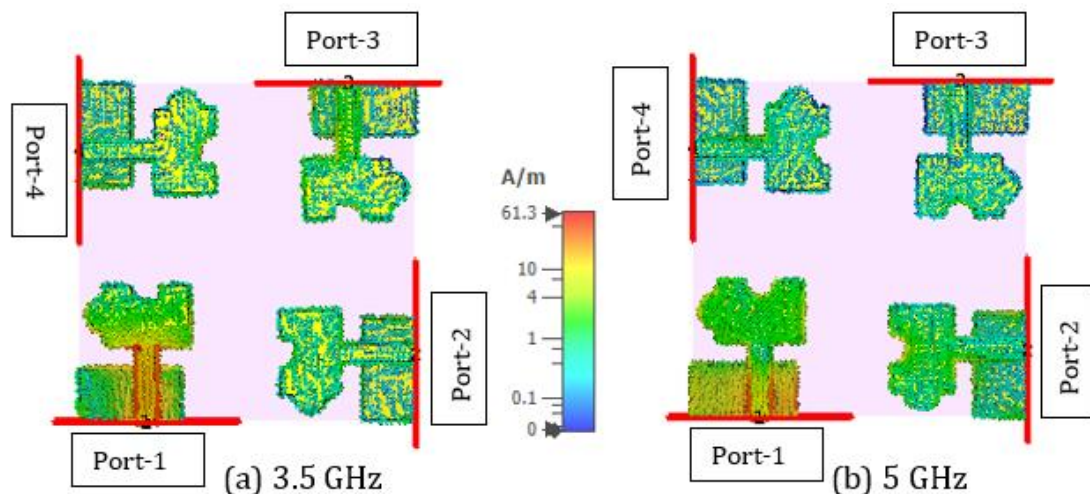


Figure 10. 3D Radiation Patterns of MIMO Antenna (a) 3.5GHz (b) 5GHz (c) 7GHz



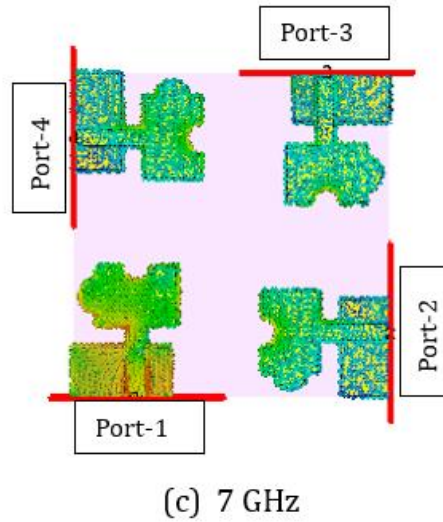


Figure 11. Surface Current Distribution of MIMO antenna

1. MIMO Performances

The parameters of MIMO antenna such as envelope correlation coefficient, diversity gain, and mean effective gain are analyzed as depicted in Fig. 12, 13, and 14.

1.1. Envelope Correlation Coefficient

The ECC can be evaluated with S parameters in equation (14):[17]

$$ECC = \frac{|S_{ii}^* S_{ij} + S_{jj}^* S_{ji}|^2}{[1 - (|S_{ii}|^2 + |S_{ij}|^2)][1 - (|S_{jj}|^2 + |S_{ji}|^2)]} \quad (14)$$

The acceptable ECC value for optimal MIMO performance is usually less than 0.5 [19]. In Figure 12, the results demonstrate that the ECC is remarkably lower than 0.0002 in the desired frequency bands.

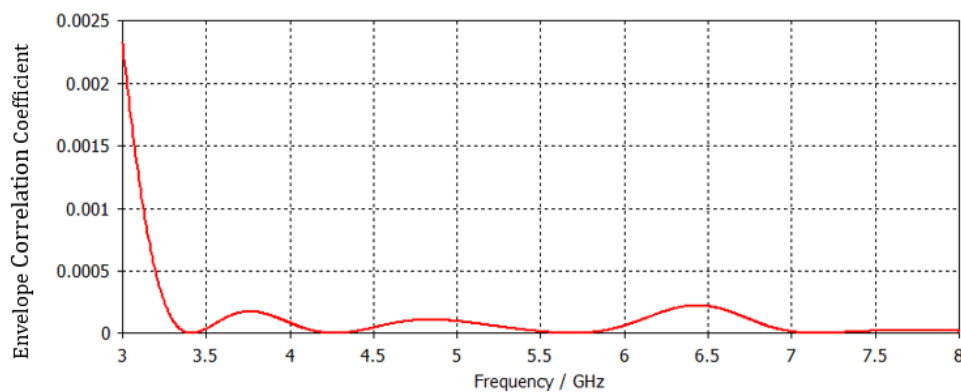


Figure 12. ECC value of MIMO Antenna

1.2. Diversity Gain

DG is evaluated according to equation (15): [17]

$$DG = 10\sqrt{1-(ECC)^2} \quad (15)$$

The $DG > 9.9$ reveals that the designed active antenna configuration has a good performance of increasing signal resiliency in MIMO systems.

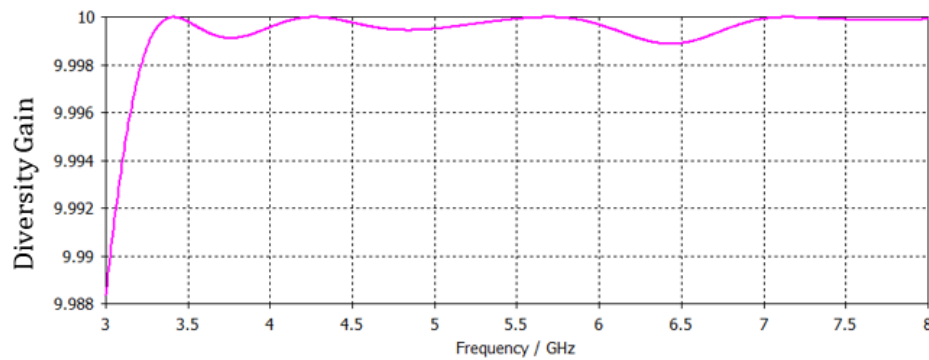


Figure 13. Diversity Gain of MIMO Antenna

1.3. Mean Effective Gain

The mean effective gain is the ratio of a power diversity antenna to an isotropic antenna. MEG is determined in Equations: (16) and (17) [18]

$$MEG_i = 0.5[1 - |S_{ii}|^2 - |S_{ij}|^2] \quad (16)$$

$$MEG_j = 0.5[1 - |S_{ij}|^2 - |S_{jj}|^2] \quad (17)$$

The satisfactory performance of mean effective gain value is desired at $-12 \text{ dB} \leq MEG \leq -3 \text{ dB}$ [19]. The value of MEG is -3 dB at the operating frequency band as demonstrated in Figure 14.

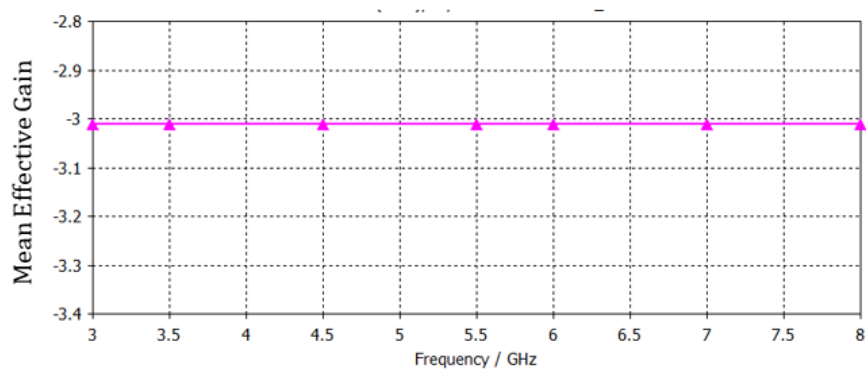


Figure 14. Mean Effective Gain of MIMO Antenna

2. Comparison with Previous Literature

MIMO antenna performance is compared with previously published literature, which is given in Table 2. It is studied that the designed MIMO antenna

has good impedance bandwidth and high isolation among all the reported MIMO antennas.

Table 2. Comparison with Previous Literature

Ref:	Size (W x L) mm	F (GHz)	Bandwidth (GHz)	MIMO Elements	Isolation dB	ECC
9	40 x 40	3.2-5.5	2.3	4	-15	0.005
10	30 x 30	4.58 - 6.12	1.54	4	<-15.4	<0.15
11	70x70	3.3-4.2	0.9	4	<-15	-
12	42x42	3.3-4.2	0.9	4	<-10	<0.04
13	136x68	3.4-3.6	0.2	4	-15	-
Proposed	40 x 40	3.3 – 8	4.7	4	<-21	<0.0002

E. Conclusion

A broadband quad-element MIMO antenna of $40 \times 40 \times 1.6$ mm³ is presented in this article. The initial single patch is structured as a semi-circular cut at the top and a semi-circle embedded at the left of the patch. These four rectangular patches are positioned orthogonally on the FR-4 substrate to achieve high isolation and a compact MIMO antenna at the desired band (3.3–8) GHz. The reported MIMO antenna has a low mutual coupling of <- 21 dB, a low envelope correlation coefficient (ECC<0.0002), a high diversity gain (DG> 9.99), an MEG gain of -3 dB, and a peak gain of 5.08 dBi. It is observed that a broadband quad-element MIMO antenna is a suitable candidate for Sub-6 GHz and Sub-7 GHz 5G applications.

F. References

- [1] W. Xiang, K. Zheng, X. Shen, "5G Mobile Communications", Springer International Publishing Switzerland, 2017.
- [2] Chow-Yen-Desmond Sim, "Novel Techniques Applied to MIMO Antenna Array for 5G Sub-7 GHz Smartphone Applications," 2023 International Workshop on Antenna Technology (iWAT), IEEE, 15-17 May 2023.
- [3] T. L. Marzetta, E. G. Larsson, H. Yang, and H. Quoc Ngo, "Fundamentals of Massive MIMO", Cambridge University Press, United Kingdom, 2016.
- [4] K. Ranjan Jha, Z. A. Pandit Jibrán, C. Singh, & S. Kumar Sharma, "4-Port MIMO Antenna Using Common Radiator on a Flexible Substrate for Sub-1GHz, Sub-6 GHz 5G NR, and Wi-Fi 6 Applications," IEEE Open Journal of Antennas and Propagation, Vol.2, pp 689-701, 26 May 2021.
- [5] S. Khan Noor, M. Jusoh, T. Sabapathy, A. Hanafiah Rambe, H. Vettikalladi, Ali M. Albishi & M. Himdi, "A Patch Antenna with Enhanced Gain and Bandwidth for Sub-6 GHz and Sub-7 GHz 5G Wireless Applications," Electronics 2023, 12, 2555.
- [6] C. Sim, Horng-Dean Chen, J. Kulkarni, Jeng-Jr Lo, Yu-Chieh Hsuan, "Recent Designs to Achieving Wideband MIMO Antenna for 5G NR Sub-6GHz Smartphone Applications," International Symposium on Antennas and Propagation, 2021.
- [7] W. Wang, "A Dual-Band Antenna Design for 5G Smartphone Applications" UK, Europe, China Millimeter Waves and THz Technology Workshop, 2018.

- [8] N.Sghaier, L. Latrach, "Design and Analysis of Wideband MIMO antenna Arrays for 5G Smartphone Application," *International Journal of Microwave and Wireless Technologies*, 2021.
- [9] N. Sheriff, S. Kamal, H. Tariq Chattha, T. Kim Geok, B. A. Khawaja, "Compact Wideband Four-Port MIMO Antenna for Sub-6 GHz and Internet of Things Applications," *Micromachines*, 2022.
- [10] M. Yang, J. Zhou, "A Compact Pattern Diversity MIMO Antenna with Enhanced Bandwidth and High-isolation Characteristics for WLAN/5G/WiFi Applications," *Microwave and optical Technological Letter*, 2020;1–12, Wiley.
- [11] X. Wang, Y. Dong, "A Four-Port MIMO Antenna System for 5G Mobile Terminals," 2020 IEEE Asia-Pacific Microwave Conference (APMC).
- [12] I. Ristika Rahmi Barani, K. Lu Wong, Y.Xuan Zhang, & W-Yu Li "Low-Profile Wideband Conjoined Open-Slot Antennas Fed by Grounded Coplanar Waveguides for 4x4 5G Operation," *IEEE Transactions on Antennas and Propagation*, 2020.
- [13] M. Abdullah, Y. Ling Ban, K. Kang, O. Kwakye Kingsford Sarkodie, & M.Yang Li, "Compact 4-port MIMO Antenna System for 5G Mobile Terminal", *International Conference on Advances in Cybersecurity*, 2017.
- [14] I. Ud Din, S. Ullah, N. Mufti, R. Ullah, B Kamal & R. Ullah, "Metamaterial-Based Highly Isolated MIMO Antenna System 5G Smartphone Application", *International Journal of Communication Systems*, Wiley, November 2022.
- [15] I. Ud Din, S. Ullah, S. Iffat Naqvi, R. Ullah, S. Ullah, E. Mousa Ali, & M. Alibakhshikenari, "Improvement in the Gain of UWB Antenna for GPR Applications by Using Frequency-Selective Surface", *International Journal of Antennas and Propagation*, Vol 2022, Article ID 2002552, Hindawi.
- [16] C. A. Balanis, "Antenna Theory, Analysis, and Design," 4th edition, John Wiley & Sons, New York, 2016.
- [17] A.A. Ibrahim, W.A.E.Ali, M.Alathbah, & A.R. Sabek, "Four-Port 38 GHz MIMO Antenna with High Gain and Isolation for 5G WirelessNetworks," *Sensors* 2023, 23, 3557.
- [18] O. Khan, S.Khan, S. Nawaz Khan MarwaMarwat, N. Gohar, M. Bilal, M. Dalarsson, "A Novel Densely Packed 4×4 MIMO Antenna Design for UWB Wireless Applications," *Sensors* 2023, 23, 8888.
- [19] A.Kumar Singh, S. Kumar Mahtoa & R. Sinh, "Quad element MIMO antenna for LTE/5G (sub-6 GHz) applications," *Journal Of Electromagnetic Waves and Applications*, 7 May 2022.